

# Imaging tumor colonization with an oncolytic Vaccinia virus strain (GLV-1h68) in a melanoma model by $^{19}\text{F}$ MRI

Thomas Christian Basse-Lüsebrink<sup>1,2</sup>, Stephanie Weibel<sup>2</sup>, Elisabeth Hofmann<sup>2</sup>, Johanna Langbein<sup>2</sup>, Volker Jörg Friedrich Sturm<sup>1</sup>, Thomas Kampf<sup>1</sup>, Peter Michael Jakob<sup>1</sup>, and Aladár Szalay<sup>2,3</sup>

<sup>1</sup>Experimental Physics 5, University of Würzburg, Würzburg, Bavaria, Germany, <sup>2</sup>Biochemistry, University of Würzburg, Würzburg, Bavaria, Germany, <sup>3</sup>Genelux Corporation, San Diego, CA, United States

## Introduction

In recent years, it was shown that oncolytic virus strains such as attenuated vaccinia virus (VACV) provide great therapeutic potential in the treatment of cancer (1). Furthermore, clinical phase 1 trials with oncolytic VACV were successfully performed (2). Importantly, the infection of tumors with viral agents often induces massive inflammation within the tumor microenvironment (1). In the past,  $^{19}\text{F}$  markers have shown their potential for unambiguously visualizing inflammation in vivo using  $^{19}\text{F}$  MRI (3,4). Thus, the purpose of study was to monitor in vivo inflammation by employing  $^{19}\text{F}$  3D MRI in a vaccinia virus treated melanoma model and to compare the spatial  $^{19}\text{F}$  patterns to non-infected controls. Furthermore, ex vivo  $^{19}\text{F}$  MRI and immunohistochemistry were performed to verify in vivo results.

## Materials and Methods

Human 1936-MEL melanoma cells were implanted on day 0 on the right limb of athymic nude mice. Nine days after tumor implantation, the attenuated VACV strain GLV-1h68 was injected i.v. into tumor-bearing animals (n = 3). Control animals received the same volume of PBS (n = 3). At days 13/4 and 15/6 after tumor cell implantation/virus injection (or PBS injection), a perfluoropolyether PFC emulsion (20% v/v, 100µl each injection) was administered i.v..

MRI was performed on a 7T small animal scanner using a home-built birdcage coil adjustable to both resonance frequencies. In vivo  $^1\text{H}$  3D turbo-spin-echo (TSE) and  $^{19}\text{F}$  3D TSE experiments were performed 17/8 days after tumor cell implantation/virus injection (or PBS injection). In vivo MRI parameters:  $^1\text{H}$ : TE/TR: 30/1000ms, Res: 0.2mm<sup>3</sup>; TF: 10; NA: 1,  $^{19}\text{F}$ : TE/TR: 4/1000ms, Res: 0.625mm<sup>3</sup>; TF: 48; NA: 60).

After in vivo MRI, the mice were sacrificed and the tumors excised. Ex vivo  $^1\text{H}/^{19}\text{F}$  3D TSE was performed ( $^1\text{H}$ : TE/TR: 81/1000ms, Res: 0.2mm<sup>3</sup>; TF: 20; NA: 1,  $^{19}\text{F}$ : TE/TR: 5/1000ms, Res: 0.625mm<sup>3</sup>; TF: 64; NA: 450).

For immunohistochemistry, tumors were fixed with 4% paraformaldehyde/PBS and cryo-sectioned into 15 µm slices. Monocytes and tissue macrophages were labeled with anti-CD68. Neutrophils were labeled with anti-Ly-6G antibodies. The labeled tissue sections were analyzed using stereo-fluorescence microscopy.

## Results

Fig. 1 shows the in vivo results. Both, VACV injected and PBS injected animals showed  $^{19}\text{F}$  signal located in the tumor. In PBS injected animals, the  $^{19}\text{F}$  signal was often spread out through the entire tumor with little signal intensity. In VACV injected animals, however, the  $^{19}\text{F}$  signal was located with high signal intensity mainly at the tumor margins. Fig. 2 provides the ex vivo MRI results of control (PBS) and VACV infected tumors. The GFP signal showed that the virus colonized in tumors of VACV injected animals. Furthermore, the  $^{19}\text{F}$  MRI signal distribution corresponded well to the histological staining pattern of macrophages (CD68) and neutrophils (Ly-6G).

## Discussion and Conclusion

VACV infected tumors showed a massive inflammation with CD68-positive macrophages and Ly-6G-positive neutrophils which accumulated in the tumor periphery. Importantly, a similar signal pattern was detected by in vivo  $^{19}\text{F}$  MRI allowing noninvasive detection of the virus induced immune cell recruitment. In PBS-injected controls accumulation of the PFC could be caused by the resident macrophage population in combination with the tumor specific enhanced permeability and retention (EPR) effect (5). Thus, it has been previously reported that  $^{19}\text{F}$  signal can be found in well perfused tumor regions after intravenous injection of PFC emulsion (6). The present study shows that PFC enhanced  $^{19}\text{F}$  MRI has great potential in the context of oncolytic cancer therapy. Besides indirectly detecting viral tumor colonization, the visualization of immune cell recruitment by  $^{19}\text{F}$  MRI may offer a new prognostic method to evaluate therapy success.

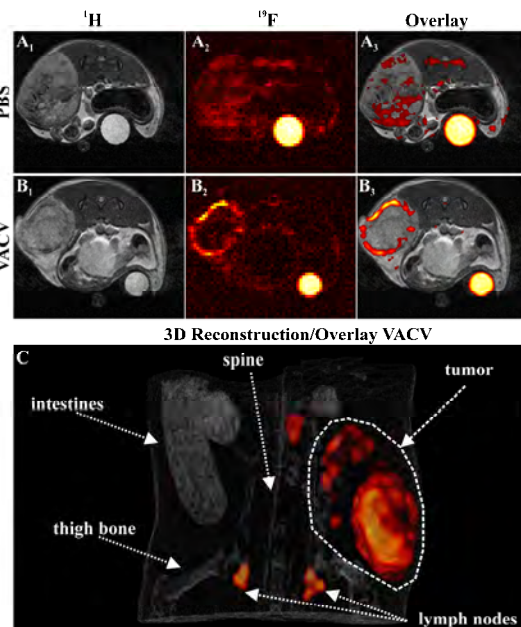


Fig.1 Results from in vivo experiments. A<sub>1-3</sub>) PBS injected animal; From left to right:  $^1\text{H}$  anatomical reference,  $^{19}\text{F}$  raw image, overlay of both images. B<sub>1-3</sub>) VACV injected animal; From left to right:  $^1\text{H}$  anatomical reference,  $^{19}\text{F}$  raw image, overlay of both images. C) 3D overlay reconstruction of a VACV injected animal (other animal as shown in A).

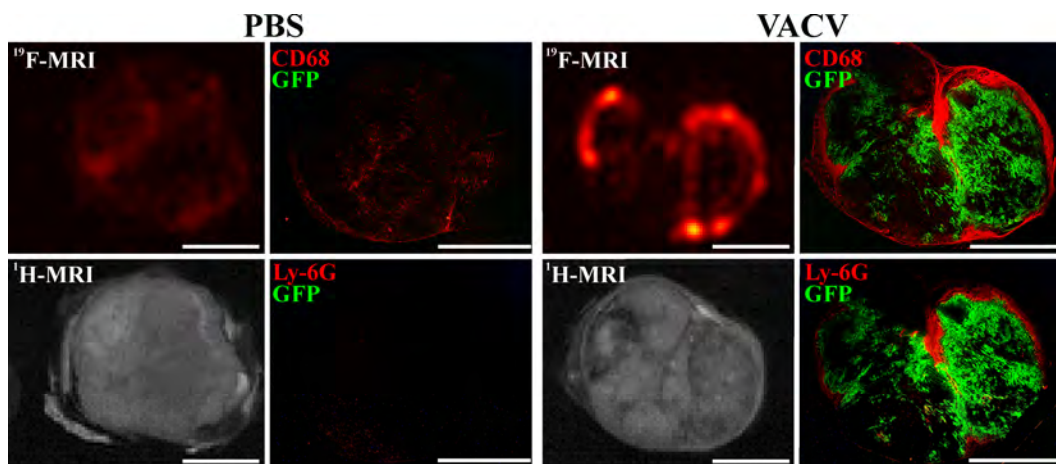


Fig.2) Ex vivo MRI and immunohistochemistry results. The scale bars represent 5mm. Ex vivo MRI data from a PBS injected animal exhibiting almost no intratumoral  $^{19}\text{F}$  signal using in vivo  $^{19}\text{F}$  MRI is shown (different animal as Fig.1B). Furthermore, ex vivo MRI of the VACV-infected animal shown in Fig.1C is provided. Tissue sections were labeled with anti-CD68 (macrophages) or anti-Ly-6G (neutrophils) antibodies. The GFP signal pattern corresponds to VACV-infected cells.

## References

- [1] Weibel S. et al., BMC Cancer (2011); 11:68:1471-2407
- [2] Pedersen J.V. et al, NCRI Cancer Conference (2010), p.C122
- [3] Nöth U. et al., Art. Cells, Blood Subs., and Immob. Biotech. (1997); 25(3):243-254
- [4] Floegel U. et al., Circulation (2008); 118(2):140-148
- [5] Fang J. et al., Adv. Drug Delivery Reviews (2011); 63:136-151
- [6] Yu J. et al., Current Medicinal Chemistry (2005); 12:819-848

## Acknowledgements

This work was supported by grants from Genelux Corporation (R&D facility in San Diego, CA, USA). AAS is salaried employee of Genelux Corporation and has personal financial interest in Genelux Corporation.